L-dopa co-drugs in nanostructured lipid carriers: A comparative study

Rita Cortesi [a], *, Elisabetta Esposito [a], Markus Drechsler [b], Gabriella Pavoni [a], Ivana Cacciatore [c], Maddalena Sguizzato [a], Antonio Di Stefano [c]

[a] Department of Life Sciences & Biotechnology, University of Ferrara, Ferrara, Italy
[b] Bayreuth Institute for Macromolecular Research (BIMF) – Soft Matter Electron Microscopy, University of Bayreuth, Germany
[c] Department of Pharmacy, University of "G. D'Annunzio" Chieti-Pescara, Italy

ARTICLE INFO

ABSTRACT

This paper describes the production and characterization of nanostructured lipid carriers (NLC) containing four different levodopa (LD) co-drugs (PD), named PDA (3,4-diacetyloxy-LD-caffeic acid co-drug), PDB (lipoic acid-dopamine co-drug), PDC (lipoic acid-3,4-diacetoxy-dopamine co-drug), and PDD (dimeric LD co-drug containing an alkyl linker), with therapeutic potential in Parkinson's disease. These co-drugs were produced with the aim of prolonging the pharmacological activity of LD, enhancing its absorption and protecting it from metabolism. These compounds were characterized by very low water solubility that limits their systemic administration. To improve the solubility of these LDPD, NLC were considered.

The obtained NLC showed acceptable particle size and a good stability up to two months from preparation. Cryo-TEM morphological characterization revealed no substantial differences between unloaded and co-drug loaded NLC. *In vitro* studies showed that the LDPD loaded NLC provided a controlled drug release. Moreover, the enhancement of LDPD stability on the hydrolysis catalysed by foetal calf serum (FCS) esterases or in the presence of lipases was evaluated as compared to a labrasol solution. In presence of esterases PDA-NLC and PDD-NLC showed half-lives higher > 3-fold as compared to the corresponding aqueous micellar solution. In the case of PDB-NLC it was found that the stability exceeds the 19 h. It can be concluded that NLC represent good strategies to encapsulate lipophilic LD co-drugs, although further studies aimed to deeply evaluate anti-parkinsonian effects *in vivo* have to be carried on.

© 2016 Published by Elsevier Ltd.

1. Introduction

Neurodegenerative disorders, such as Alzheimer's and Parkinson's diseases, are a heterogeneous group of disorders characterized by progressive and selective loss of anatomically or physiologically related neuronal systems [1,2]. The majority of these diseases affect patients later in life, even if abundant evidence suggests the existence of a "preclinical" stage that could start years before a subject can be diagnosed [3].

Notably, Parkinson's disease is a chronic and progressive disorder of the nervous system affecting movement and precisely the brain neurons producing dopamine [4–6]. As Parkinson's disease progresses, the amount of dopamine produced in the brain decreases, leaving a person unable to control its movement. Parkinson's disease symptoms include muscle rigidity, tremors and changes in speech and gait. After diagnosis, treatments can help relieve symptoms, but they are not resolutive. Current therapy for Parkinson's disease is essentially actuated with levodopa (LD), a direct precursor of dopamine [5]. Although LD is the treatment of choice, its metabolism generates a variety of free radicals that contribute to the progression of the disease, increasing the loss of nigrostriatal dopaminergic neu-

rons [6]. Complications are associated with LD long-term therapy [7].

Miller et al. confirmed that catecholamines, including dopamine and LD, are subjected to autoxidation [8]. This process is enhanced by the presence of neuromelanin in dopaminergic neurons, with production of potentially cytotoxic reactive oxygen species (ROS) [9]. Indeed ROS have been hypothesized to play a role in the progressive and selective loss of nigrostriatal dopaminergic neurons that occurs in neurodegenerative disorders such as Parkinson's disease [10]. This hypothesis suggests that the inhibition of catecholamine's autoxidation and the scavenging of ROS produced by such oxidation are important strategies for preventing or slowing down the progression of aging and aged-related neurodegenerative disorders.

Starting from these data, Di Stefano and colleagues, using both the direct- and linker co-drug strategies, synthesized several co-drugs obtained by joining antioxidant molecules to therapeutic compounds as potential tools for the treatment of neurodegenerative disease such as Parkinson's and Alzheimer's diseases [11–13]. In this context, they also developed dimeric prodrugs in which two identical molecules were joined together through a dicarboxylic chain that, after administration, underwent to metabolism guaranteeing a sustained release of the drug [14].
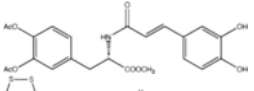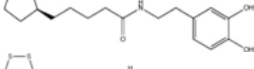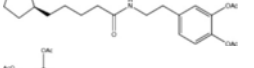
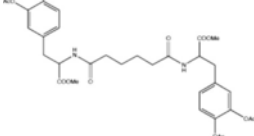In this study four LD co-drugs (PD), namely PDA, PDB, PDC, and PDD, previously synthesized by Di Stefano and colleagues [11,13,14], were selected and subjected to further study (Table 1). PDA was synthesized through the interaction of 3,4-diacetyloxy-

* Corresponding author at: Department of Life Sciences and Biotechnology, University of Ferrara, I-44121 Ferrara, Italy.
Email address: crt@unife.it (R. Cortesi).

Table 1
Chemical structure and some physico-chemical characteristics of LDPD used in the present study.

Drug	Structure	MW	λ_{max} (nm)	Log P	Melting point (°C)
PDA		429.2	254	2.29	140
PDB		341.3	282	3.65	80
PDC		397.4	220	3.40	60
PDD		630.3	220	0.92	170

L-dopa methyl ester hydrochloride with caffeic acid. Preliminary *in vitro* and *in vivo* studies evaluated chemical and enzymatic properties of this molecule and showed that PDA is stable in aqueous solutions and improves the release of LD and dopamine in the brain [11].

PDB and PDC were obtained by linking dopamine to (*R*)-α-lipoic acid, a well-known antioxidant and iron-chelating agent. PDB and PDC were synthesized by classical synthetic methodology through the interaction of (*R*)-α-lipoic acid with 2-(3,4-dihydroxy)-phenylethylamine and 2-(3,4-diacetoxy)-phenylethylamine, respectively. These multifunctional co-drugs could represent useful dopaminergic agents devoid of the pro-oxidant effects associated with the presence of the catechol moiety [13].

Finally, PDD, prepared by coupling reaction between 3,4-diacetyloxy-L-phenylalanine methyl ester hydrochloride with hexanedioyl dichloride, showed chemical stability in aqueous, acid, and physiological solutions [14]. However, all LD co-drugs, reported in this study, showed poor water solubility.

To date, many nanotechnology-based approaches were developed to increase solubility, reduce plasma fluctuations, and improve the blood brain permeability of drugs [15]. Solid lipid nanoparticles, micelles, liposomes are currently used to enhance solubility of drugs and to protect drugs by enzymatic degradation thus improving their bioavailability and guaranteeing tissue-targeted delivery [16,17]. Notably, for the treatment of Parkinson's disease, chitosan nanoparticles with dopamine adsorbed onto the external surface [18], lactoferrin-modified nanoparticles encapsulating human neurotrophic factor gene [19], and formulation of LD loaded microspheres [20] were recently developed with the aim to prevent drug degradation and obtain a sustained release of the intact compound enhancing dopamine levels in rat brain affected by Parkinson's disease.

Here we describe a possible strategy to allow the improvement of solubility of our co-drugs based on nanostructured lipid carriers (NLC), that have attracted significant attention due to their potential application as matrixes able to improve the bioavailability of active molecules [16,21]. Moreover, lipid nanosystems have been recently proposed for the therapy of brain diseases [22–24] offering clinical advantages such as reduction of drug dosage and side effects, increased drug viability, and improved patient quality of life [25]. Particularly, an emerging approach employed to circumvent the blood brain barrier (BBB) is the use of colloidal carriers [26–29], which allow brain penetration to non-transportable drugs by masking their physico-chemical characteristics. Ubiquinone-, apomorphine-, and idebenone-loaded nanostructured lipid carriers were developed as

drug delivery systems for the treatment of neurodegenerative pathologies [30–31]. Taking account of these assumptions, the present paper will describe the preparation, characterization, *in vitro* studies and preliminary *in vivo* evaluation of NLC containing four different PD with therapeutic potential in Parkinson's disease.

2. Materials and methods

2.1. Materials

Tristearin, stearic triglyceride (tristearin) was provided by Fluka (Buchs, Switzerland). Miglyol 812N, caprylic/capric triglycerides (tricaprylin) was a gift of Cremer Oleo Division (Witten, Germany). Lutrol F 68, methyl-oxirane polymer (75:30) (poloxamer 188) was a gift of BASF ChemTrade GmbH (Burgbernheim, Germany). Caprylocaproyl macrogol-8 glycerides (labrasol) was purchased form Gattefossé (France).

2.2. NLC preparation

NLC were prepared by stirring followed by homogenization or ultrasonication. Briefly, 1 g of lipid mixture was heated at 70 °C. The lipid mixture concentration was 5% w/w (with respect to the total weight of dispersion) and was constituted of a mixture tristearin/tricaprylin 2:1 w/w. To the melted lipid phase 19 ml of an aqueous poloxamer 188 solution (2.5% w/w) was added at 70 °C under 13,500 rpm high-speed stirrer for 1 min, using a Ultra Turrax T25 (IKA-Werke GmbH & Co. KG, Staufen, Germany). The emulsion was then subjected to ultrasonication (Microson™, Ultrasonic cell Disruptor) at 6.75 kHz for 15 min and cooled down to room temperature by placing it in a water bath at 22 °C. NLC dispersions were stored at room temperature. Each LDPD-containing NLC (NLC-PD) was prepared by adding 1 mg of LDPD to the molten lipid mixture and afterwards the aqueous phase was added.

2.3. Characterization of NLC

2.3.1. Photon correlation spectroscopy (PCS)

Submicron particle size analysis was performed using a Zetasizer 3000 PCS (Malvern Instr., Malvern, England) equipped with a 5 mW helium neon laser with a wavelength output of 633 nm. Glassware was cleaned of dust by washing with detergent and rinsing twice with water for injections. Measurements were made at 25 °C at an angle of 90°. Data were interpreted using the "method of cumulants" [32].

2.3.2. Cryo-transmission electron microscopy (cryo-TEM)

For cryo-TEM studies, a sample droplet of 2 µl was put on a lacey carbon filmed copper grid (Science Services, Munich), which was hydrophilized by air plasma glow discharge (Solarus 950, Gatan, Munich, Germany) for 30 s. Subsequently, most of the liquid was removed with blotting paper leaving a thin film stretched over the lace holes. The specimens were instantly shock frozen by rapid immersion into liquid ethane cooled to approximately 90 K by liquid nitrogen in a temperature-controlled freezing unit (LEICA EM GP, Germany). The temperature was monitored and kept constant in the chamber during all the sample preparation steps. The specimen was inserted into a cryotransfer holder (CT3500, Gatan, Munich, Germany) and transferred to a Zeiss/LEO EM922Omega EFTEM (Zeiss Microscopy GmbH, Jena, Germany). Examinations were carried out at temperatures around 90 K. The TEM was operated at an acceleration voltage of 200 kV. Zero-loss filtered images (DE = 0 eV) were taken under reduced dose conditions (100–1000 e/nm²). All images were registered digitally by a bottom mounted CCD camera system (Ultra-

scan 1000, Gatan, Munich, Germany) combined and processed with a digital imaging processing system (Digital Micrograph GMS 1.9, Gatan, Munich, Germany).

2.3.3. Water and dispersed phase loss after NLC production

The disperse phase that was lost on the paddle of the overhead mechanical stirrer was recovered and weighed. The dispersions were then weighed to evaluate the water evaporation due to high temperature and rapid stirring during production. The water loss due to evaporation was calculated using Eq. (1).

$$waterloss = WTTPsol2.5\% - (Wdp + Wdisp)$$ (1)

where W TTP sol 2.5% is the weight of the lipidic mixture (tristearin/tricaprylin 2:1 w/w) and the aqueous Poloxamer 188 solution, Wdp is the weight of disperse phase lost on the paddle and Wdisp is the weight of dispersion after production. An amount equal to the lost water was then added to the preparation to restore the optimal conditions.

2.4. Drug content of dispersions

With the aim to quantify the total drug content (free plus bonded) of dispersions after production, a sample of dispersion was diluted (1:4 v/v) in methanol and stirred for 3 h in order to completely extract the drug. Then, the sample was filtered through 0.45 μm membrane pore diameter and analysed by HPLC for drug content, as detailed below.

$$Drug\ recovery = \frac{drugdetected \times 100}{totaldrug}$$ (2)

All data were the mean of 8 determinations on different batches of the same type of dispersion.

The HPLC determinations were performed using a two-plunger alternative pump (Jasco, Japan), an UV-detector operating at 254 nm and a 7125 Rheodyne injection valve with a 50 μl loop. 40 μl samples were loaded on a stainless steel C-18 reverse-phase column (15 × 0.46 cm) packed with 5 μm particles (Grace® – Alltima RP 18, Alltech, USA).

Elution was performed with a mobile phase constituted of methanol and water (60:40 v/v) at a flow rate of 0.5 ml/min. In these conditions, the retention time of LD-PD was 5.4 min.

2.5. Stability studies

Stability studies on physical aspect and size of NLC dispersions were conducted in triplicate at day 0, 10, 30 and 60 from production of formulations. Physical stability studies were performed analysing macroscopic aspect (phase separation, turbidity, macroscopic viscosity) under visual inspection.

To predict long-term stability, samples were stored in glass vials at 25 °C for 2 months [33–34]. Chemical stability was evaluated determining PD content by HPLC analyses.

Log (PD residual content, %) was plotted against time and the slopes (m) were calculated by linear regression. The slope (m) was then substituted into the Eq. (3) for the determination of rate constant values k:

$$k = m \times 2.303$$ (3)

Shelf life values (the time for 10% loss, t_{90}) were then calculated using the Eq. (4).

$$t_{90} = 0.105/k$$ (4)

2.6. In vitro studies

2.6.1. Release kinetics

In vitro release tests were carried out using the dialysis method. Typically, 5 ml of NLC dispersion were placed into a dialysis tube (10 cm; molecular weight cut off 10.000–12.000, Medi Cell International, UK), then placed into 100 ml of receiving phase constituted of water and ethanol (50:50 v/v) and shaken in a horizontal shaker (MS1, Minishaker, IKA, Germany) at 175 rpm at 37 °C. For comparison each co-drug was solubilized in water and ethanol (50:50 v/v) in the free form and subjected to dialysis. At regular time intervals, namely, 0, 30 min, 1 h, 2 h, 3 h, 4 h, 5 h, 6 h, 7 h, 8 h and 24 h, 400 μl samples of receiving phase were withdrawn and refilled again with fresh medium mixture. Afterwards, samples were diluted with methanol in a 1:1 v/v rate. The amount of drug released was determined by HPLC as described above.

The obtained release data were fitted to semi-empirical equations describing Fickian, diffusional and dissolutive release mechanisms, respectively [35]:

$$M_t/M_\infty = K_{diff} t^{1/2} + c'$$ (5)

$$1 - M_t/M_\infty = e^{-K_{diss} t} + c$$ (6)

stated that M_t is the drug fraction released at the time t; M_∞ is the total drug content of the analysed NLC; K, c and c′ are coefficients calculated by plotting the linear forms of the indicated equations.

It is well known that Fick's law of diffusion describes a solute transport from polymeric or lipid matrices. In particular Fickian diffusion refers to the solute transport process in which the matrix relaxation time (tr) is much greater than the solvent diffusion time (td). The mathematical modelling simplifies the release process and gains insight into the release mechanisms of a specific material system.

2.6.2. Nanoparticle degradation in the presence of esterases or lipases

Thirteen test tubes containing 100 μl of NLC-PDA dispersion or PDA containing labrasol micelle solution were added to 100 μl of foetal calf serum (10% v/v) aqueous solution. Afterwards they were placed in a thermostatic bath at 37 °C. At different time intervals, comprised between 0 and 24 h (1440 min), samples were removed from the bath and added of 150 μl of pure methanol. Samples were filtered with 0.22 μm nylon filters (Spartan 13, Whatman, Germany) and analysed by HPLC as described above. A kinetic curve was obtained plotting the amounts of non-degraded PDA as a function of time.

To test lipases effect, eight sample containing 400 μl of NLC, 400 μl of Palizsch buffer ($Na_2B_4O_7$ 5 mM; NaCl 18 mM; H_3BO_3 180 mM) and 200 μl of swine pancreatic type II lipases were prepared. The experiment was conducted in bath thermostated at 37 °C. Samples were taken at predetermined time intervals (from 30 min up to 8 h). Subsequently 250 μl of each sample was added to 500 μl of methanol. Afterwards samples were filtered with 0.22 μm nylon fil-

ters (Spartan 13, Whatman, Germany) and analysed by HPLC as described above.

2.7. Data analysis and statistics

Statistical analysis was performed by the analysis of variance (ANOVA), followed by SPSS 11.5. The level of significance was taken at P-values < 0.05.

3. Results and discussion

3.1. Production and characterization of lipid dispersions

The NLC were obtained by dispersing the lipid phase in the aqueous phase under sonication, as previously described [36], to obtain stable and homogenous dispersions. Particularly, it is known that the use of the liquid oil tricaprylin in mixture with solid lipids leads to the formation of solid carriers with homogenous lipid nanocompartments [36–40]. From the evaluation of the water and dispersed phase loss it was found that the loss of water was 0.93% while the loss of lipid disperse phase on the vessel was around 4% w/w with respect to the weight of lipid phase before dispersion. On the other hand the presence of large particles was < 1% with respect to the total weight of disperse phase. Thus the method of preparation did not heavily affect the total quantity of dispersed nanoparticles and, consequently, the encapsulation efficiency of the drug.

Four synthesized LD co-drugs, named PDA, PDB, PDC, and PDD, were used as model drugs (Table 1). After production, nanoparticles were characterized in terms of morphology and dimensions. Size and distribution of the produced NLC were determined using the photon correlation spectroscopy (PCS). The analyses were made immediately after preparation and periodically at regular intervals for 2 months, in order to investigate the stability of nanoparticles by time.

In Table 2 are reported the values of mean diameters and polydispersity obtained within two months. It should be noted that in general no variations of the diameters occurs by time and there is no difference in size between NLC with or without the drug, except for NLC-PDB probably linked to a lower drug encapsulation efficiency.

Concerning the polydispersity indexes no variations were observed indicating that LDPD-containing NLC remain quite stable maintaining their size over time.

Cryo-TEM allowed an investigation of the inner structure of nanosized formulations, empty and LDPD-containing. Fig. 1 reports cryo-TEM images of the produced NLC dispersions, namely NLC-PDA, NLC-PDB, NLC-PDC and NLC-PDD.

The panels show circular and elongated or irregular shaped platelet-like particles. More or less round shaped platelets are imaged in top view. When a platelet is tilted perpendicular, the side view of the particle is visible showing dark rod-like structures. Sometimes the inner ultrastructure is visible showing several layers [38–41] resembling disk-like bicelles [42–43]. If the platelets are only tilted to some degree elliptically shaped or rice-like features are visible [36, 37]. All views from top view to side view can be visualized by tilting the whole sample in the cryo-TEM with the help of the goniometer stage. Spindle-like particles would not change their shape upon tilting and could not be detected (results not shown). Moreover, some cap- or spoon-like structures are visible similar to nano-spoons or nano-brooms related to platelets in side view which have small amounts of oily lipid (i.e. tricaprylin particles on their surfaces [37]. No differences in term of morphology are evident for the shown preparations.

As indicated in Table 2, it has to be noticed that the nanoparticle diameter is slightly affected by the presence of LD derivatives. Indeed in some cases the drug increased the percentage of larger nanoparticles as demonstrated by the polydispersity index. However, the polydispersity indexes remain quite stable during the length of time considered [32]. The small size (< 200 nm) of the prepared nanoformulations could permit them to cross the blood brain barrier and reach the damaged area of the brain affected by Parkinson's disease [44,45]. Moreover, due to the small size, these lipid nanocarriers could escape from the reticuloendothelial system [46] guaranteeing an increased metabolic resistance and consequently prolonged half-life of the PD co-drugs.

3.2. Efficiency of drug encapsulation

The amount of drug encapsulated in NLC with respect to the total amount used for the preparation, was evaluated by high-performance liquid chromatography (HPLC) using a reversed-phase column as described in the Experimental section. As reported in Table 3, drug recovery after NLC production was higher than 70% as compared to the total amount used for the preparation, except for PDB. Indeed, the drug encapsulation was 72.91% in the case of NLC-PDA, 75.31% in the case of PDC, and 81.87% in the case of NLC-PDD dispersions. NLC-PDB showed a drug incorporation of 24.57% ± 5.89, probably due to the loss of the active substance during the preparation procedure, especially during the addition to the lipid phase to the poloxamer aqueous solution.

Shelf life stability was calculated plotting Log (PD residual content, % with respect to drug content at time 0) against time, obtaining first order kinetics (data not shown). From the slopes (m), obtained by linear regression, shelf life values (t_{90}), i.e. the time at which the drug concentration has lost 10%, were calculated and reported in Table 3.

It was found that PDB shows 90% of PD stability for 3 days, PDA for 35 days, PDC for 74 days and PDD up to 82 days.

3.3. In vitro experiments

In order to obtain information on drug release from NLC and to compare them, the dialysis method was used. The obtained results are summarized in Fig. 2. It can be observed that all the produced NLC formulations provide a controlled release of the encapsulated drug. In particular, after the first hour NLC-PDA and NLC-PDB released the 20% of total drug content, while NLC-PDC and NLC-PDD released a higher amount being 25–30%. In all cases, after 24 h, the drug released reached almost 70% of total drug content. These data suggest
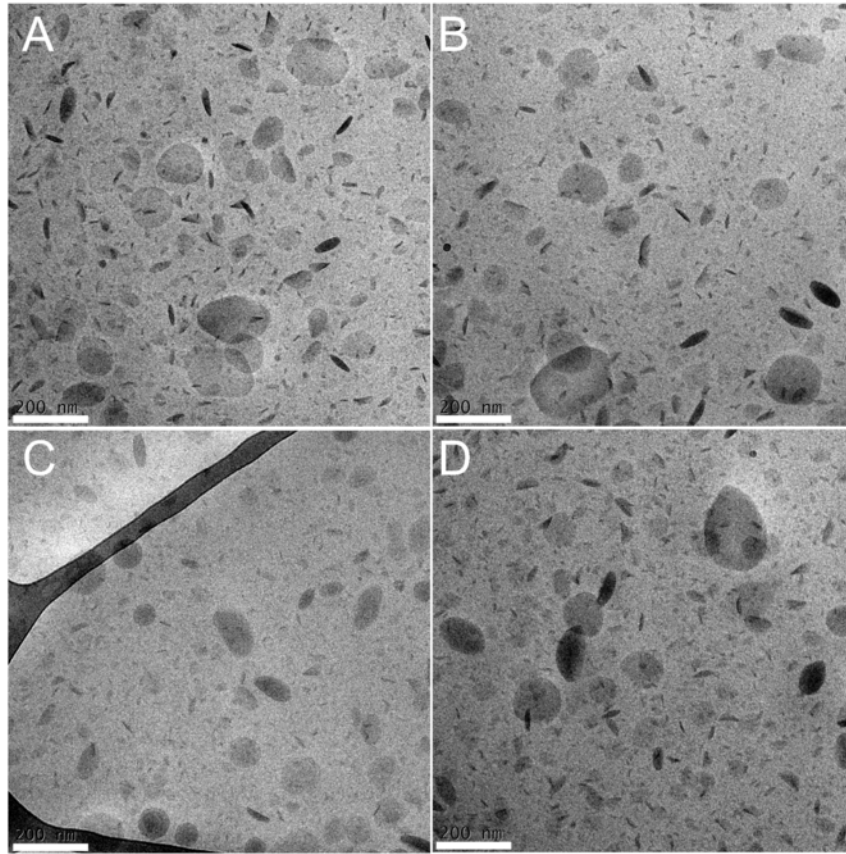
Table 2
Mean diameters of NLC as determined by PCS.

Day	empty	PDA	PDB	PDC	PDD
	Z ave (nm) P.I.	Z ave (nm) P.I.	Z ave (nm) P.I.	Z ave (nm) P.I.	Z ave (nm) P.I.
0	191.5 ± 3.7 *0.11*	197.0 ± 2.1 *0.20*	180.? ± 1.0 *0.36*	188.5 ± 2.9 *0.22*	194.1 ± 2.1 *0.21*
10	193.8 ± 1.6 *0.16*	193.7 ± 2.1 *0.22*	n.d. /	n.d. /	196.6 ± 1.6 *0.21*
30	192.1 ± 5.5 *0.19*	192.3 ± 0.8 *0.25*	186.9 ± 1.? *0.35*	189.6 ± 1.3 *0.27*	188.6 ± 0.5 *0.25*
60	188.2 ± 0.9 *0.24*	186.6 ± 1.1 *0.21*	186.8 ± 5.2 *0.25*	182.8 ± 0.8 *0.24*	186.8 ± 3.5 *0.20*

s.d. = standard deviation calculated after 5 determinations on different batches of the same type of dispersion; n.d. = non determined; P: polydispersity index.

Fig. 1. Cryo-transmission electron microscopy (cryo-TEM) images of the produced NLC dispersions NLC-PDA (panel A), NLC-PDB (panel B), NLC-PDC (panel C) and NLC-PDD (panel C). Bar indicates 200 nm.

Table 3
PD content in NLC as a function of time.

	PDA	PDB	PDC	PDD
PD recovery (%)[a]				
t_0	72.91 ± 5.45	24.75 ± 5.89	75.31 ± 6.68	81.87 ± 8.67
t_{30}	68.04 ± 3.67	10.18 ± 2.28	72.48 ± 6.32	78.42 ± 4.
t_{60}	61.07 ± 3.25	3.42 ± 1.88	69.20 ± 3.94	75. ± 5.87
Shelf life values				
K	0.00295	0.03299	0.00141	.0012
t_{90} (days)[b]	35.54	3.18	74.44	

The reported results represent the average of four independent experiments ± S

[a] As a function of initial CLO content.

[b] Time at which the drug concentration has lost 10%.

that the obtained nanoformulations could improve the controlled release and the targeting of the entrapped LD co-drugs [43].

The theoretical release curves mimicking a dissolutive and a diffusive model were determined according to the linear form of Eqs. (4) and (5), respectively [33].

In Fig. 3 the comparison between the theoretical curves calculated from the above reported equations and the experimental curves obtained for NLC are reported. Table 4 reports the release kinetic parameters obtained from the different LDPD from the produced NLC. The obtained R and R^2 values indicate that the experimental curves are superimposable to the theoretical ones referring to dissolutive kinetics, apart from PDC-NLC characterized by a diffusive kinetic (R = 0.96557). The similarity of R values obtained by Eqs. (4) and (5) suggests that both mechanisms could occur together resulting in a

mixed release of dissolutive and diffusive type. The slight prevalence of one over the other could be tentatively attributable to the strength of the interaction of the LDPD with the lipid matrix.

3.3.1. Effect of esterase and lipases

It is well known that a co-drug (being a prodrug) is an inactive (or significantly less active) molecule that once administered is metabolised *in vivo* into an active metabolite [47–49]. Taking into consideration this definition, this study evaluate the quantity of co-drug non-degraded, and thus the quantity of the LDPD released after *in vitro* activity of esterases/lipases used to mimic the *in vivo* metabolisation. Moreover this experiment could allow us to possibly estimate if the inclusion of LDPD in NLC induces an enhancement in the stability of LDPD as compared to a labrasol solution on the hydrolysis catalysed by foetal calf serum (FCS) esterases or in the presence of lipases.

To support this, the LDPD with lowest log P were considered, namely PDA and PDD. Fig. 3 reports the comparative effect of FCS esterases on the selected LDPD in NLC and in micellar solution (labrasol 5% w/v) during 24 h. The values of half-time degradation were extrapolated by graphs and reported in Table 5. It is noteworthy that both PDA-NLC and PDD-NLC showed half-lives > 3-fold higher (*i.e.* 3.40 and 3.02, respectively) as compared to the corresponding aqueous micellar solution. These data confirm that the nanoformulations, protecting the entrapped LD co-drugs by plasma esterases, could ensure prolonged half-life and tissue-targeted delivery of the LD co-drugs.
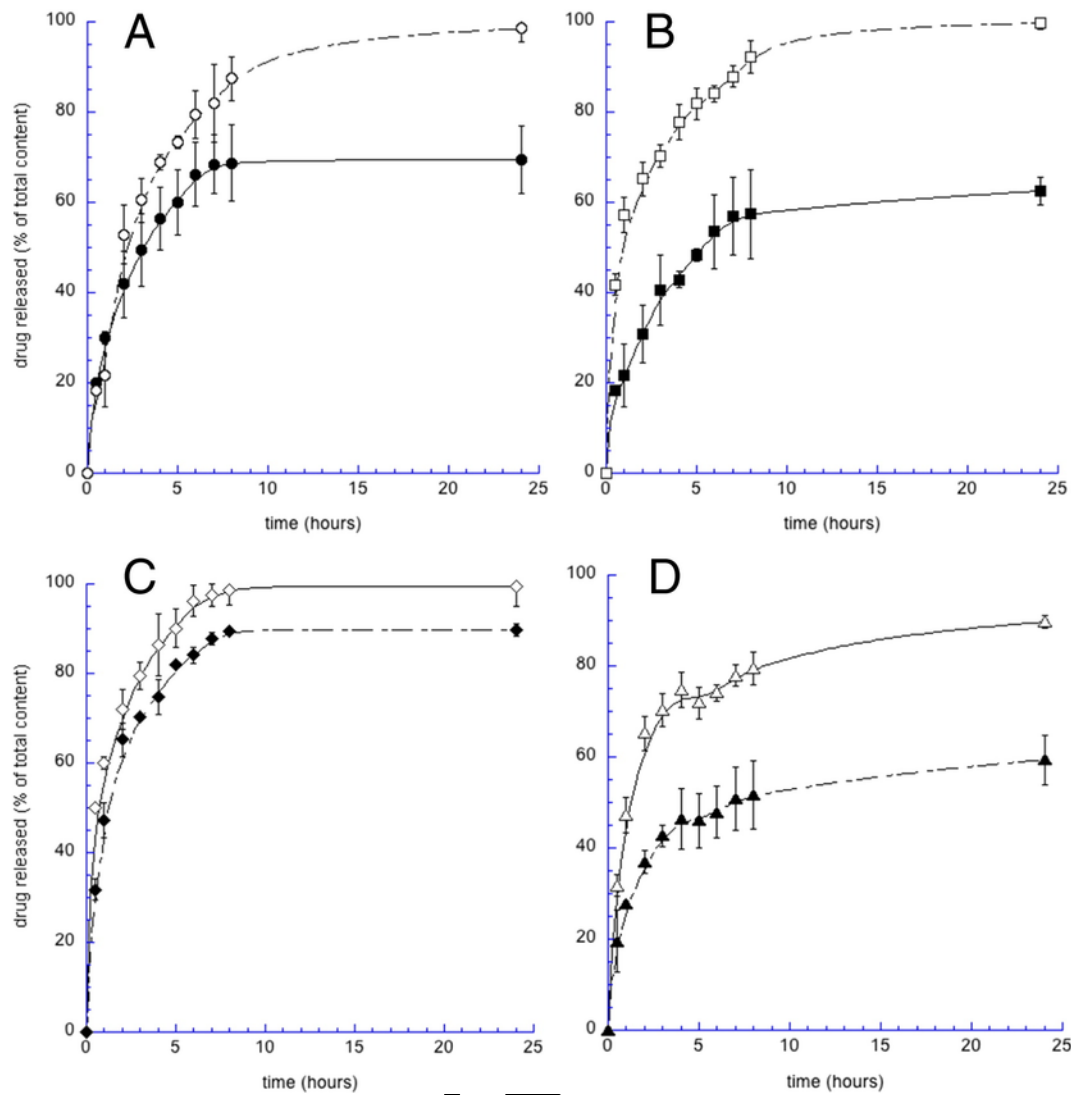
Fig. 2. Dialysis release of LDPD from NLC (black symbols) and as free form (white symbols). Panel A: PDA (circles). Panel B: PDB (squares). Panel C: PDC (diamonds). Panel D: PDD (triangles). Data are the mean of 6 independent experiments ± s.d.

Concerning lipases, experiments were conducted on PDA-NLC, PDB-NLC, PDC-NLC and PDD-NLC. The results are reported in Fig. 4 and Table 5. From the analyses of data it emerges that for PDA-NLC the half-time degradation is almost superimposable to that of esterases, while for PDD-NLC the increase in stability doubled that of esterases. Notwithstanding, in the case of PDB-NLC and PDC-NLC a comparison with esterase activity was not possible, it is evident that the stability of the co-drug is very long since it exceeds the 19 h (1156 min). Moreover, as expected due to their analogue chemical structure, the effect of lipases on PDB-NLC and PDC-NLC was very similar (Fig. 5).

4. Conclusions

The low solubility of LD derivatives in aqueous solution represents one limitation for oral administration. To ameliorate it, significant amounts of surfactants have to be used resulting in a possible *in vivo* toxicity [50–52]. In this view, the chance to administrate LD derivatives using lipid nanoparticles could be very useful and interesting. It was demonstrated that the inclusion of LDPD within lipid nanoparticles could improve the solubility allowing for a reduction of the dosage. Moreover, in a previous study performed using NLC-PDA as model formulation, we demonstrated the potential usefulness of this type of formulation [38]. *In vivo* tests demonstrated that NLC-PDA replicated the therapeutic benefit of LD, with a slightly reduced maximal effect but a longer lasting action (up to 24 h) [38]. Moreover, the small size, a high entrapment efficiency, and the resistance to esterases of these nanoformulations could ensure other advantages such as improved capacity to cross the blood brain barrier, prolonged half-life, and tissue-targeted and controlled delivery of the entrapped LD co-drugs. Thus, NLC represent an intriguing tool to encapsulate lipophilic LD co-drugs, although further studies aimed to deeply evaluate anti-parkinsonian effects *in vivo* have to be carried on.
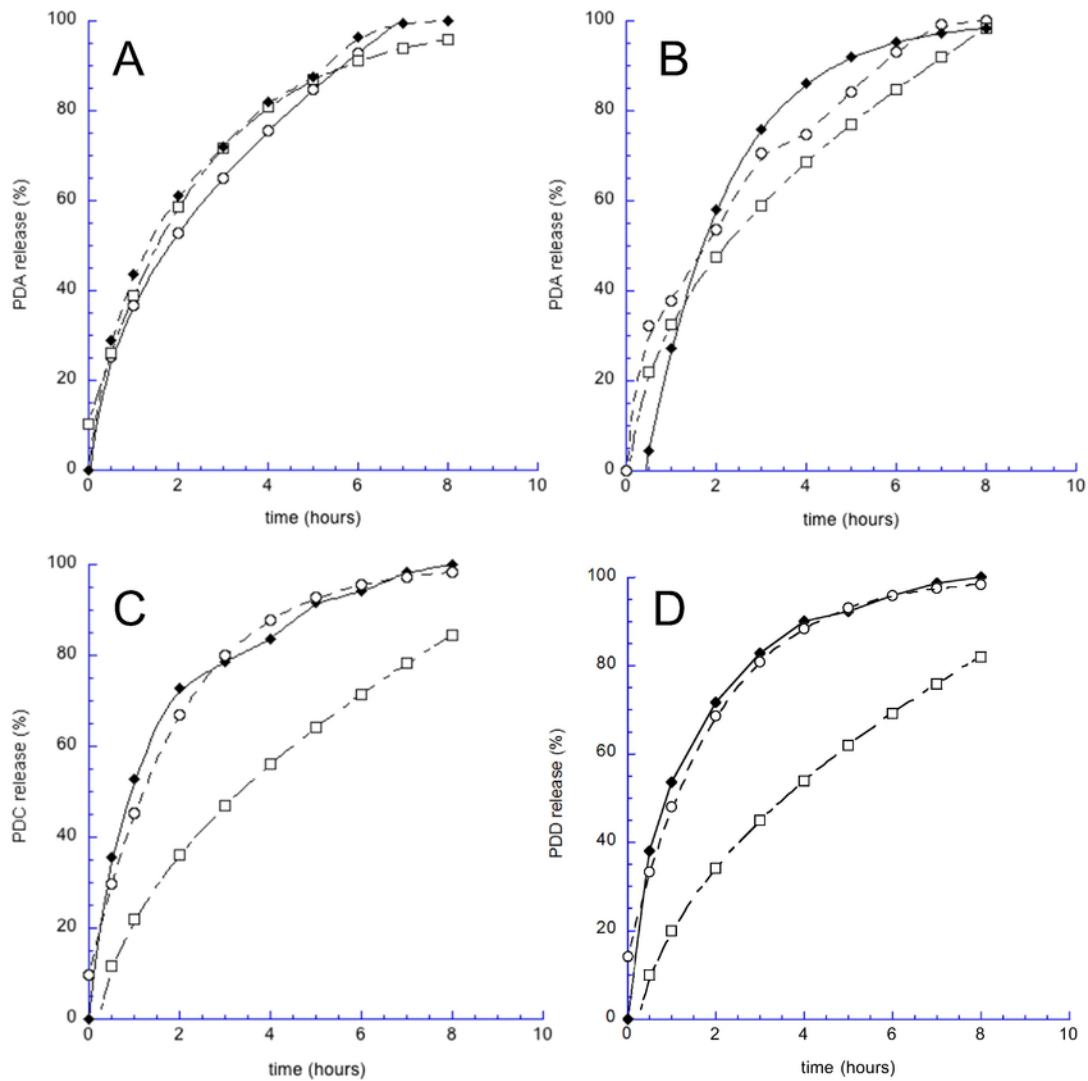
Fig. 3. Comparison of the theoretical (dotted lines) and experimental (●, solid ...LDPD profiles from NLC. The theoretical curves were obtained using the coefficient calculated by linear regression of the linearized form of Eq. (2) (squares) and Eq. (3 ...cles).

Table 4
Release kinetic parameters of drug release from the produced NLC.

Equation LD	K	c,c′	R	R²
$M_t/M_\infty = K_{diff}\, t^{0,5} + c'$				
PDA	− 0.3848	4.4953	.99645	0.99291
PDB	− 0.3931	4.8352	0.9..48	0.85042
PDC	− 0.5022	4.5..3	0.98151	0.96336
PDD	− 0.5019	4.4..25	0.96..05	0.93132
$1 - M_t/M_\infty = e^{-K_{diss}\, t} + c$				
PDA	38.842	..249.	0...756	0.99513
PDB	35.971	3.5..8	0.99602	0.99206
PDC	34.276	12.45..	0.97221	0.94519
PDD	33.939	13.905	0.96557	0.93232

K and c – Mathematical coefficients ob...ned by ...lotting the linear forms of the indicated equations; R – Regression coefficien...; ...² – Squared regression coefficient.

Table 5
Effect of the esterases and lipases towards the codrugs encapsulated on NLC (half-time degradation).

	Esterases T ½ (min)	s.d.	Lipases T ½ (min)	s.d.
PDA-NLC	296	3	288	4
PDA-solution	87	2	n.d.	n.d.
PDB-NLC	n.d.	n.d.	1156	5
PDD-NLC	275	4	568	3
PDD-solution	91	2	n.d.	n.d.

The reported results represent the average of 3 independent experiments ± s.d. The codrugs were dissolved in water in the presence of labrasol 5% w/v. n.d.: not determined.
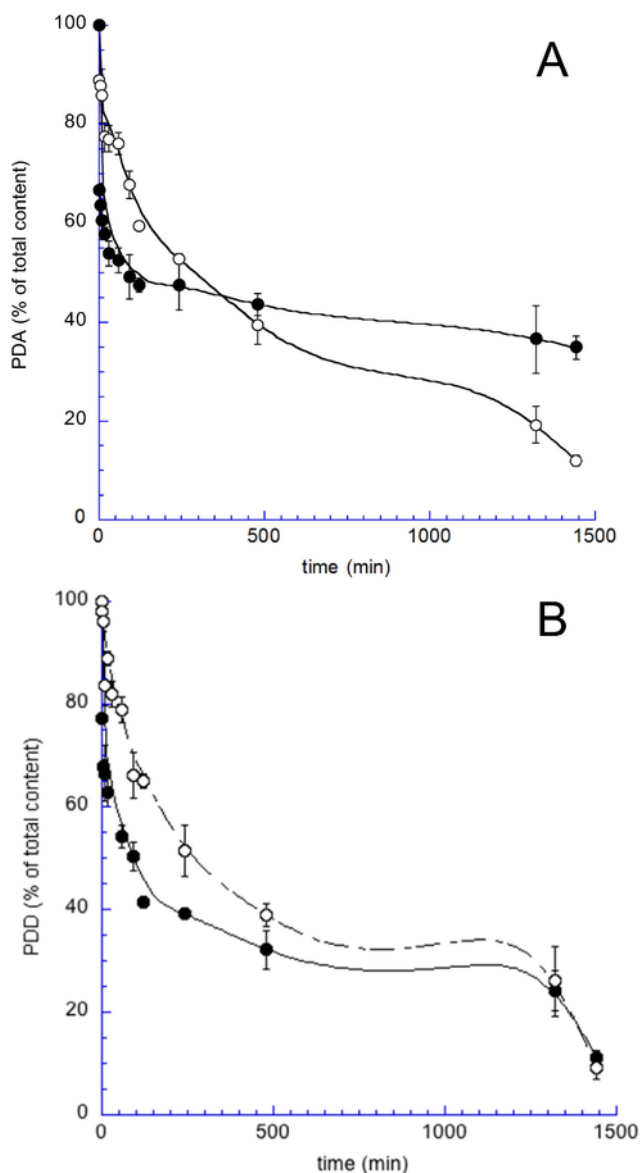
Fig. 4. Comparative effect of FCS esterases on PDA (panel A) and PDD (panel B) tested in NLC (open symbols) or in aqueous solution (labrasol 5% w/v) (closed symbol). The reported results represent the average of three independent experiments ± s.d.

Fig. 5. Effect of lipase on LDP-NLC: PDA (circles), PDB (squares), PDC (diamonds) and PDD (triangles). The results are the average of three independent experiments ± s.d.

References

[1] M.S. Forman, J.Q. Trojanowski, V.M. Lee, Neurodegenerative diseases: a decade of discoveries paves the way for therapeutic breakthroughs, Nat. Med. 10 (2004) 1055–1063.

[2] D.M. Skovronsky, V.M. Lee, J.Q. Trojanowski, Neurodegenerative diseases: new concepts of pathogenesis and their therapeutic implications, Ann. Rev. Pathol. 1 (2006) 151–170.
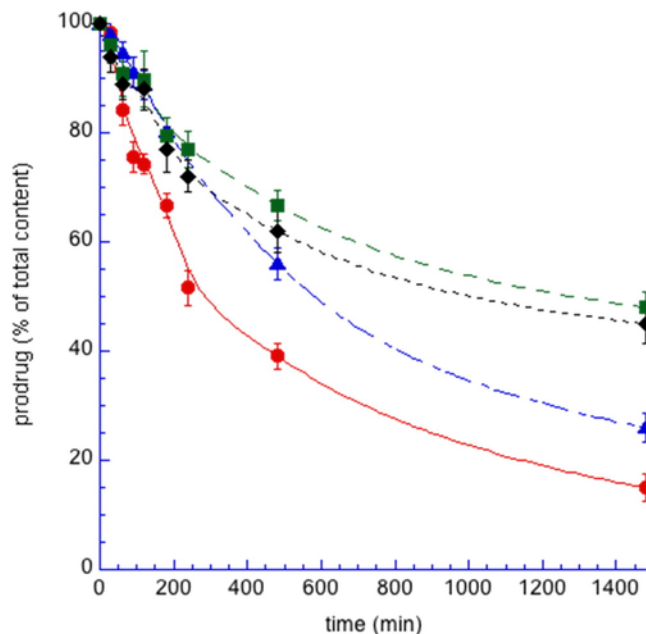
[3] I. Litvan, M. Chesselet, T. Gasser, D.A. Di Monte, D. Parker, T. Hagg, J. Hardy, P. Jenner, J.H. Myers, D. Price, M. Hallett, W.J. Langston, A.E. Lang, G. Halliday, W. Rocca, C. Duyckaerts, D.W. Dickson, Y. Ben-Shlomo, C.G. Goetz, E. Melamed, The etiopathogenesis of Parkinson disease and suggestions for future research. Part I, J. Neuropathol. Exp. Neurol. 66 (2007) 251–257.

[4] J.M. Beitz, Parkinson's disease: a review, Front. Biosci. 6 (2014) 65–74.

[5] E. Tolosa, M.J. Martí, F. Valldeoriola, J.L. Molinuevo, History of levodopa and dopamine agonists in Parkinson's disease treatment, Neurology 50 (1998) S2–S10.

[6] P.A. Serra, G. Esposito, P. Enrico, M.A. Mura, R. Migheli, M.R. Delogu, M. Miele, M.S. Desole, G. Grella, E. Miele, Manganese increases L-DOPA auto-oxidation in the striatum of the freely moving rat: potential implications to L-DOPA long-term therapy of Parkinson's disease, Br. J. Pharmacol. 130 (2000) 937–945.

[7] W.C. Koller, Neuroprotective therapy for Parkinson's disease, Exp. Neurol. 144 (1997) 24–28.

[8] J.W. Miller, J. Selhub, J.A. Joseph, Oxidative damage caused by free radicals produced during catecholamine autoxidation: protective effects of O-methylation and melatonin, Free Radic. Biol. Med. 21 (1996) 241–249.

[9] W.S. Enoch, T. Sarna, L. Zecca, P.A. Riley, The roles of neuromelanin, binding of metal ions, and the oxidative cytotoxicity in the pathogenesis of Parkinson's disease: a hypothesis, J. Neural Transm. 7 (1994) 83–100.

[10] J.D. Adams, I.N. Odunze, Oxygen free radicals and Parkinson's disease, Free Radic. Biol. Med. 10 (1991) 161–169.

[11] P. Sozio, A. Iannitelli, L.S. Cerasa, I. Cacciatore, C. Cornacchia, G. Giorgioni, M. Ricciutelli, C. Nasuti, F. Cantalamessa, A. Di Stefano, New L-dopa codrugs as potential antiparkinson agents, Arch. Pharm. 341 (2008) 412–417.

[12] F. Pinnen, I. Cacciatore, C. Cornacchia, P. Sozio, L.S. Cerasa, A. Iannitelli, C. Nasuti, F. Cantalamessa, D. Sekar, R. Gabbianelli, M.L. Falcioni, A. Di Stefano, Codrugs linking L-dopa and sulfur-containing antioxidants: new pharmacological tools against Parkinson's disease, J. Med. Chem. 52 (2009) 559–563.

[13] A. Di Stefano, P. Sozio, A. Cocco, A. Iannitelli, E. Santucci, M. Costa, L. Pecci, C. Nasuti, F. Cantalamessa, F. Pinnen, L-dopa- and dopamine-(R)-α-lipoic acid conjugates as multifunctional codrugs with antioxidant properties, J. Med. Chem. 49 (2006) 1486–1493.

[14] A. Di Stefano, B. Mosciatti, G.M. Cingolani, G. Giorgioni, M. Ricciutelli, I. Cacciatore, P. Sozio, F. Claudi, Dimeric L-dopa derivatives as potential pro-drugs, Bioorg. Med. Chem. Lett. 11 (2001) 1085–1088.

[15] H.E. Gendelmana, V. Anantharam, T. Bronichc, S. Ghaisasb, H. Jin, A.G. Kan-thasamy, X. Liua, J.E. McMillana, R.L. Mosleya, B. Narasimhan, S.K. Mal-lapragada, Nanoneuromedicines for degenerative, inflammatory, and infectious nervous system diseases, Nanomedicine 11 (2015) 751–767.

[16] I. Cacciatore, M. Ciulla, E. Fornasari, L. Marinelli, A. Di Stefano, Solid lipid nanoparticles as a drug delivery system for the treatment of neurodegenerative diseases, Exp. Opin. Drug Deliv. 13 (2016) 1121–1131.

[17] A. Di Stefano, P. Sozio, A. Iannitelli, L.S. Cerasa, New drug delivery strategies for improved Parkinson's disease therapy, Expert Opin. Drug Deliv. 6 (2009) 389–404.

[18] A. Trapani, E. De Giglio, D. Cafagna, N. Denore, G. Agrimi, T. Cassano, S. Gaetani, V. Cuomo, G. Trapani, Characterization and evaluation of chitosan nanoparticles for dopamine brain delivery, Int. J. Pharm. 419 (2011) 296–307.

[19] R. Huang, W. Ke, Y. Liu, Gene therapy using lactoferrin-modified nanoparticles in a rotenone-induced chronic Parkinson model, J. Neurol. Sci. 290 (2010) 123–130.

[20] E. D'Aurizio, P. Sozio, L.S. Cerasa, M. Vacca, L. Brunetti, G. Orlando, A. Chi-avaroli, R.J. Kok, W.E. Hennink, A. Di Stefano, Biodegradable microspheres loaded with an anti-Parkinson prodrug: an in vivo pharmacokinetic study, Mol. Pharm. 8 (2011) 2408–2415.

[21] R.H. Muller, K. Mäder, S. Gohla, Solid lipid nanoparticles (SLN) for controlled delivery-a review of the state of the art, Eur. J. Pharm. Biopharm. 50 (2000) 161–177.

[22] K. Westesen, B. Siekmann, Biodegradable colloidal drug carrier systems based on solid lipids, in: S. Benita (Ed.), Microencapsulation, Marcel Dekker, New York, 1996, pp. 213–258.

[23] J.K. Vasir, M.K. Reddy, V. Labhasetwar, Nanosystems in drug targeting: oppor-tunities and challenges, Curr. Nanosci. 1 (2005) 47–64.

[24] E. Barbu, E. Molnár, J. Tsibouklis, D.C. Górecki, The potential for nanoparti-cle-based drug delivery to the brain: overcoming the blood–brain barrier, Expert Opin. Drug Deliv. 6 (2009) 553–565.

[25] S. Pasha, K. Gupta, Various drug delivery approaches to the central nervous sys-tem, Expert Opin. Drug Deliv. 7 (2010) 113–135.

[26] E. Garcia-Garcia, K. Andrieux, S. Gil, P. Couvreur, Colloidal carriers and blood–brain barrier (BBB) translocation: a way to deliver drugs to the brain?, Int. J. Pharm. 298 (2005) 274–292.

[27] J.J. Wang, K.S. Liu, K.C. Sung, C.Y. Tsai, J.Y. Fang, Lipid nanoparticles with different oil/fatty ester ratios as carriers of buprenorphine and its prodrugs for injection, Eur. J. Pharm. Sci. 38 (2009) 138–146.

[28] R.H. Müller, Lipid nanoparticles: recent advances, Adv. Drug Deliv. Rev. 59 (2007) 522–530.

[29] M.D. Joshi, R.H. Müller, Lipid nanoparticles for parenteral delivery of actives, Eur. J. Pharm. Biopharm. 71 (2009) 161–172.

[30] B.K. Nanjwade, V.T. Kadam, F.V. Manvi, Formulation and characterization of nanostructured lipid carrier of ubiquinone (Coenzyme Q10), J. Biomed. Nan-otechnol. 9 (2013) 450–460.

[31] C.L. Fang, S.A. Al-Suwayeh, J.Y. Fang, Nanostructured lipid carriers (NLCs) for drug delivery and targeting, Recent Pat. Nanotechnol. 7 (2013) 41–55.

[32] R. Pecora, Dynamic light scattering measurement of nanometer particles in liq-uids, J. Nanopart. Res. 2 (2000) 123–131.

[33] J.I. Wells, Pharmaceutical Preformulation: The Physicochemical Properties of Drug Substances, Ellis Horwood, Chichester, England, 1988.

[34] V. Agrahari, S. Putty, C. Mathes, J.B. Murowchick, B.-B.C. Youan, Evaluation of degradation kinetics and physicochemical stability of tenofovir, Drug Test. Anal. 7 (2015) 207–213.

[35] E. Esposito, E. Menegatti, R. Cortesi, Hyaluronan based microspheres as tools for drug delivery: a comparative study, Int. J. Pharm. 288 (2005) 35–49.

[36] E. Esposito, M. Fantin, M. Marti, M. Drechsler, L. Paccamiccio, P. Mariani, E. Sivieri, F. Lain, E. Menegatti, M. Morari, R. Cortesi, Solid lipid nanoparticles as delivery systems for bromocriptine, Pharm. Res. 25 (2008) 1521–1530.

[37] K. Jores, W. Mehnert, M. Drechsler, H. Bunjes, C. Johann, M. Kale, Investiga-tions on the structure of solid lipid nanoparticles (SLN) and oil-loaded solid lipid nanoparticles by photon correlation spectroscopy, field-flow fractionation and transmission electron microscopy, J. Control. Release 95 (2004) 217–227.

[38] L. Ravani, M.G. Sarpietro, E. Esposito, A. Di Stefano, P. Sozio, M. Calcagno, M. Drechsler, C. Contado, F. Longo, M.C. Giuffrida, F. Castelli, M. Morari, R. Cortesi, Lipid nanocarriers containing a levodopa prodrug with potential an-tiparkinsonian activity, Mater. Sci. Eng. C 48 (2015) 294–300.

[39] Y. Yang, A. Corona III, B. Schubert, R. Reeder, M.A. Henson, The effect of oil type on the aggregation stability of nanostructured lipid carriers, J. Colloid In-terface Sci. 418 (2014) 261–272.

[40] N. Naseri, H. Valizadeh, P. Zakeri-Milani, Solid lipid nanoparticles and nanos-tructured lipid carriers: structure, preparation and application, Adv. Pharm. Bull. 5 (2015) 305–313.

[41] E. Esposito, L. Ravani, M.S. Drechsler, P. Mariani, C. Contado, J. Ruokolainen, P. Ratano, P. Campolongo, V. Trezza, R. Nastruzzi, R. Cortesi, Cannabinoid an-tagonist loaded in nanostructured lipid carriers (NLCs): design, characterization and in vivo study, Mater. Sci. Eng. C 48 (2015) 328–336.

[42] U.H.N. Dürr, R. Soong, A. Ramamoorthy, When detergent meets bilayer: birth and coming of age of lipid bicelles, Prog. Nucl. Magn. Reson. Spec-trosc. 69 (2013) 1–22.

[43] C.R. Sanders, R. Scott Prosser, Bicelles: a model membrane system for all sea-sons?, Structure 6 (1998) 1227–1234.

[44] M. Masserini, Nanoparticles for brain drug delivery, ISRN Biochem. (2013), 238428 (18 pages).

[45] E. Esposito, H.E. Drechsler, M.A. van der Pol, F. Boschi, L. Calderan, S. Man-nucci, M. Drechsler, C. Contado, R. Cortesi, C. Nastruzzi, Production, physico-chemical characterization and biodistribution studies of lipid nanoparticles, J. Nanomed. Nanotechnol. 6 (2015) 1.

[46] P.J. White, F. Anastasopoulos, C.W. Pouton, B.J. Boyd, Overcoming biological barriers to in vivo efficacy of antisense oligonucleotides, Expert. Rev. Mol. Med. 11 (2009) e10.

[47] N. Das, M. Dhanawat, B. Dash, R.C. Nagarwal, S.K. Shrivastava, Codrug: an efficient approach for drug optimization, Eur. J. Pharm. Sci. 41 (2010) 571–588.

[48] J. Rautio, H. Kumpulainen, T. Heimbach, et al., Prodrugs: design and clinical applications, Nat. Rev. Drug Discov. 7 (2008) 255–270.

[49] K.M. Huttunen, H. Raunio, J. Rautio, Prodrugs–from serendipity to rational de-sign, Pharmacol. Rev. 63 (2011) 750–771.

[50] E. Lémery, S. Briançon, Y. Chevalier, C. Bordes, T. Oddos, A. Gohier, M.-A. Bolzinger, Skin toxicity of surfactants: structure/toxicity relationships, Colloid Surf. A 469 (2015) 166–179.

[51] M. Lavorgna, C. Russo, B. D'Abrosca, A. Parrella, M. Isidori, Toxicity and genotoxicity of the quaternary ammonium compound benzalkonium chloride (BAC) using Daphnia magna and Ceriodaphnia dubia as model systems, Envi-ron. Pollut. 210 (2016) 34–39.

[52] J. Misik, E. Vodakova, R. Pavlikova, J. Cabal, L. Novotny, K. Kuca, Acute toxi-city of surfactants and detergent-based decontaminants in mice and rats, Mil. Med. Sci. Lett. 81 (2012) 171–176.